Effects of simulated rare earth recycling wastewaters on biological nitrification

Yoshiko Fujita,[*,1] Joni Barnes,[1] Ali Eslamimanesh,[2] Malgorzata M. Lencka,[2] Andrzej Anderko,[2] Richard E. Riman,[3] and Alexandra Navrotsky[4]

[1]Idaho National Laboratory, Idaho Falls, ID 83415
[2]OLI Systems Inc., 240 Cedar Knolls Road, Suite 301, Cedar Knolls, NJ 07927
[3]Rutgers, The State University of New Jersey, Department of Materials Science and Engineering, 607 Taylor Road, Piscataway, NJ 08855
[4]Peter A. Rock Thermochemistry Laboratory and NEAT ORU, University of California Davis, Davis CA 95616

ABSTRACT

Current efforts to increase domestic availability of rare-earth element (REE) supplies by recycling and expanded ore processing efforts will result in increased generation of associated wastewaters. In some cases disposal to a sewage treatment plant may be favored but plant performance must be maintained. To assess the potential effects of such wastewaters on biological wastewater treatment, model nitrifying organisms *Nitrosomonas europaea* and *Nitrobacter winogradskyi* were exposed to simulated wastewaters containing varying levels of yttrium or europium (10, 50 and 100 ppm), and the REE extractant tributyl phosphate (TBP, at 0.1 g/L). Y and Eu additions above 10 ppm inhibited *N. europaea* activity, even when initially virtually all of the REE was insoluble. The provision of TBP together with Eu increased inhibition of nitrite production by the *N. europaea*, although TBP alone did not substantially alter nitrifying activity. *N. winogradskyi* was more sensitive to the simulated wastewaters, with even 10 ppm Eu or Y inducing significant inhibition, and a complete shutdown of nitrifying activity occurred in the presence of the TBP. To analyze the availability of REEs in aqueous solutions, REE solubility has been calculated using the previously developed MSE (Mixed-Solvent Electrolyte) thermodynamic model. The model calculations reveal a strong pH dependence of solubility, which is typically controlled by the precipitation of REE hydroxides but may also be influenced by the formation of a phosphate phase.

Introduction

The increased global demand for rare earth elements (REE) and other elements highly valued for their role in many renewable energy and other advanced technologies (e.g., magnets for wind turbines, electric vehicles, smart phones) has led to increased exploration for new REE sources and also interest in new methods for ore processing and refining, as well as for recycling of materials containing these strategic metals. [1] The expansion of REE production industries will be accompanied by growing volumes and new compositions of wastewater. Companies will have to develop acceptable practices for safe disposal of these wastestreams. Waste disposal methodologies can have a large impact on process design, costs and sustainability. For some industrial generators, sending aqueous wastestreams to a municipal wastewater treatment plant, or Publicly Owned Treatment Works (POTW), may be a cost effective disposal option. However, wastewaters that jeopardize the performance of the POTW will not be acceptable. In particular, upset of biological wastewater treatment is a major concern. Biological wastewater treatment, mediated

by highly efficient microbial communities adapted for this purpose, is a critical module in modern POTWs, enabling them to meet requirements for discharge to water bodies such as oceans, lakes or rivers.

Currently there are scant data regarding the impact of REEs on biotic systems in general, and federal pretreatment standards for REE process wastewaters introduced into a POTW (40 CFR 421.275) do not include any standards for REEs themselves. Most of the reported studies examining the effects of REE on microbes have focused on biosorption of REE,[2-7] often as analogues for trivalent actinides.[8, 9] However, there are some early qualitative studies that showed REE to be toxic to both bacteria and fungi.[10] In addition, high concentrations of cerium nitrate have been shown to inhibit the growth of Gram negative bacteria and fungi in the treatment of burn wounds[11] and negative]effects on soil microbes has been reported following the use of REE containing fertilizers in China.[12] As a result, researchers have used *E. coli* to explore the antimicrobial mechanisms of REEs and have reported toxicity at high concentration of Ce, La and Pr.[13-16]

Biological wastewater treatment typically comprises both aerobic and anaerobic biological processes, and for the aerobic module the activated sludge process is the most commonly used treatment practice.[17] A critical function of activated sludge treatment is nitrification, which consists of the oxidation of ammonia to nitrite (reaction 1), and then the subsequent oxidation of nitrite to nitrate (reaction 2) by a different set of bacteria.

$$NH_3 + 1.5O_2 \rightarrow NO_2^- + H^+ + H_2O \quad (1)$$

$$NO_2^- + 0.5O_2 \rightarrow NO_3^- \quad (2)$$

Both ammonia and nitrite oxidizers are generally slow growing organisms that are sensitive to a variety of external factors including temperature, pH, dissolved oxygen and chemical toxins such as heavy metals[18-20] and a myriad of organic compounds including phenols, hydrocarbons and halogenated hydrocarbons.[21, 22] As a result, the nitrifying activity of activated sludge is more vulnerable to inhibition than other microbial conversions and, due to the slow growth rate of nitrifying bacteria, recovery of damaged sludge can be time consuming and costly. For these reasons, pure cultures of nitrifying bacteria are frequently used to assess the inhibitory effects of industrial and pharmaceutical wastewaters on biological treatment systems. [23-25]

In this report, we present results from aerobic pure culture studies using two nitrifying bacterial species, *Nitrosomonas europaea* and *Nitrobacter winogradskyi*, which were exposed to REE. *N. europaea* is an ammonia oxidizer, and *N. winogradskyi* is a nitrite oxidizer. The bacterial cultures were challenged with synthetic wastewaters containing yttrium or europium. These REEs were chosen because they would be targeted for recovery during recycling of fluorescent light phosphor powders; residuals would be expected to remain in wastewater generated during the recycling process. Phosphor recycling has been identified as having significant potential for near-term commercial recovery of REEs, due to the high content of Y, Eu and Tb in fluorescent lamp phosphors, the large volume of lamps already in use, and the existing infrastructure of end-of-life recycling services. [1] Hence, if phosphor recycling is implemented at industrial scale, POTWs may well receive increasing loads of wastewaters generated by phosphor REE recyclers. In addition to the REEs, we tested the effects of an organic complexant, tributyl phosphate (TBP), a common solvent used for the extraction of REE from aqueous solutions.

The cultures of the nitrifying bacteria were exposed to varying levels of either Y or Eu and effects on nitrification activity (production of nitrite for the *N. europaea*, and consumption of nitrite for *N. winogradskyi*) were measured as a function of time. In addition, experiments were conducted in the presence or absence of the complexant TBP. Because of the high viscosity of TBP (3.399 mPa·s at 25°C; [26]), it is typically used in solvent extraction as a mixture with an alkane solvent; for our experiments we utilized 30:70 mixture (v/v) of TBP and the isoparaffin solvent Isopar™ L.

In order to understand the effects of experimental conditions (e.g., pH, total REE concentration and the presence of TBP) on the nitrification processes, it is important to predict the availability of dissolved REEs in aqueous solutions as a function of those experimental conditions. Such predictions can be obtained from a thermodynamic model provided that the model is accurately parameterized to reflect solution speciation including acid-base equilibria, complexation and precipitation of solid phases. Although various kinetically-controlled phenomena (e.g., slow precipitation of solid phases or adsorption on cell surfaces) can influence the availability of REEs, equilibrium solubility provides a foundation for understanding the behavior of REEs.

A suitable framework for such calculations is provided by the previously developed Mixed-Solvent Electrolyte (MSE) model.[27, 28] This model combines an equation of state for standard-state properties of individual species, an excess Gibbs energy model, and an algorithm for solving phase and chemical equilibria in multiphase systems. Although there is a scarcity of well-documented thermodynamic solubility data in the open literature for Eu and Y in acidic and TBP-containing solutions, the MSE framework[27, 28] enables us to leverage the available data and make reasonable predictions.

Materials and Methods

Chemicals. Unless specified otherwise, all chemicals used were ACS reagent grade. Yttrium oxide (99.99%) was purchased from Research Chemicals (Phoenix, AZ) and europium chloride (99.99%) from Strem Chemicals, Inc. (Newburyport, MA). Tributyl phosphate was provided within a commercial isoparaffin matrix (Isopar™ L, from ExxonMobil), as a 30:70 (v/v) mixture.

Bacterial cultures. *Nitrosomonas europaea (ATCC 19718)* and *Nitrobacter winogradskyi (ATCC 25391)* cultures were both obtained from the American Type Culture Collection. The *N. europaea* strain was routinely cultivated in a defined mineral medium specifically developed for this organism and described by Sato et al.[29] The *N. winogradskyi* strain was routinely cultivated in medium described by Soriano and Walker.[30] Both cultures were grown at 30°C in the dark with rotary shaking (100 rpm).

Synthetic wastewater composition. The synthetic wastewater consisted of Y_2O_3 or $EuCl_3$ dissolved in 0.1 M HCl, at concentrations of 0, 10, 50, and 100 ppm of the respective metal. In some of the challenge experiments, TBP in Isopar™ L was included at final concentration of 100 ppm as TBP (lower than 400 ppm which is the approximate solubility of TBP in water at 25°C).[31] Therefore, no liquid phase split is expected throughout the experiments.

REE and TBP exposure experiments. The experiments were conducted in 250 ml culture flasks with closures designed to allow air exchange. Abiotic control experiments were included alongside the biotic experiments. To each flask, 15 ml of the synthetic wastewater (containing REE at final concentrations of 0, 10, 50 and ppm) were added. Then, because in an activated sludge system with nitrification the

optimum pH is generally between 7 and 8,[32] the pH was adjusted to pH 7.5-8.0 with NaOH. Next, 60 ml of either the Sato et al. medium[29] (for *N. europaea* experiments) or the Soriano and Walker medium[30] (for *N. winogradskyi* experiments) were added to each flask. For the biotic experiments, the medium was pre-inoculated (5% v/v) with 48 h cultures of the bacterial strains (~2.0×10^7 cells/mL for *N. europaea*; ~1.5×10^7 cells/mL for *N. winogradskyi*). The final concentrations of the rare earths were 0, 10, 50 and 100 ppm. The effects of TBP were also tested on each culture, along with the Isopar^{TM} L alone. For the *N. europaea*, TBP (100 ppm) was also tested together with Eu to determine if synergistic effects occurred. For the *N. winogradskyi*, TBP (100 ppm) was provided together with Y. Biotic treatment flasks were set up in triplicate, with one abiotic control for each experimental condition. The flasks were incubated at 30°C in the dark, with shaking (100 rpm). At 0, 24, 48 and 72 h, samples (2 ml) were taken for pH and nitrite measurements. At 72 hours, samples (10 ml) were collected for measurement of REE content.

Analytical methods. Nitrite was measured colorimetrically using American Public Health Association Standard Method 4500-NO_2-B.[33] REE concentrations were measured using inductively coupled plasma mass spectrometry (ICP-MS). The instrument (iCAP Q, Thermo Scientific) was standardized and operated in accordance with manufacturer instructions. Ultrapure concentrated nitric acid was used to acidify (1%) the filtered (0.22 micron pore size) samples as well as the commercial standard stock solutions prior to ICP-MS analysis.

Thermodynamic speciation calculations. The solubilities of Y and Eu in the synthetic aqueous solutions were predicted using the MSE thermodynamic model.[27, 28] This model is described in the Supporting Information. The parameters of the MSE model[27, 28] have been determined by analyzing and regressing the available thermodynamic data. Table 1 shows the sources of the experimental data, data types, temperature, pressure and ranges of REE distribution coefficient data.

An important constraint in the data regression was the fact that the available data for the Y/Eu + TBP + acid + H_2O solutions are limited to a few sets of distribution coefficients for the REE between the aqueous phase and the organic (TBP-rich) phase. Therefore, the first step in the analysis was to determine the model parameters that represent the liquid-liquid equilibrium (LLE) data for the TBP + acid + H_2O systems. For this purpose, the experimental LLE data for the TBP + HNO_3/HCl/$HClO_4$ aqueous solutions have been regressed to obtain the necessary interaction parameters.

The second step was to represent the solubility data for various inorganic REE species including hydroxides, chlorides, and phosphates. Since the REE hydroxides are likely to precipitate rapidly (compared to measurement time) in the media investigated in this work, we focused on the determination of parameters to account for the solubility of $Y(OH)_3$ and $Eu(OH)_3$. To the best of our knowledge, the only relevant data in the open literature for $Y(OH)_3$ and $Eu(OH)_3$ are the solubility products (K_{sp}) for the freshly precipitated and aged hydroxides in various aqueous solutions. To obtain reproducible and predictive thermodynamic parameters, the solubility products for aged REE hydroxides have been chosen and regressed. The sources of these data are tabulated in Table 1.

It has been well established in the literature that TBP forms neutral complexes with REEs with the general formula of $REEA_mTBP_n$ in which A is an anion, and m and n are the stoichiometric ratios depending on the chemical solvation mechanism for the extraction of an REE in a specific system.[34-36] Such complexes play a key role in extraction-based separation processes. One of the dominant anions in the media studied here that has, at the same time, the potential to take part in a complex with TBP is the

chloride ion. However, only one data point has been found in the literature pertaining to the distribution of Eu between an HCl-containing aqueous phase and a TBP organic phase[37] whereas there are more abundant data sets for the Y/Eu + HNO_3/$HClO_4$ aqueous solutions with TBP. Therefore, data for various systems have been combined to obtain the best estimates of complexation parameters. The methodology that was adopted to determine the required model parameters is described in the Supporting Information. The thermodynamic model parameters that were derived and or used in this study are also presented in the Supporting Information, in Tables S1-S4.

Results and Discussion

Effects of REEs on ammonia oxidation by **N. europaea**. Activity of the *N. europaea* cultures was monitored by measuring production of nitrite over time; other researchers have reported that nitrite production correlates well with microbial growth for *N. europaea*, [29, 38] and this was confirmed in preliminary experiments conducted in our laboratory (data not shown). No nitrite production was detected in any of the abiotic controls, and therefore such data are not shown in the figures or discussed further.

Data for nitrite production over the course of the experiments exposing *N. europaea* to 10, 50, and 100 ppm Eu are presented in Figure 1a. The results indicated that Eu at 10 ppm had little or no impact on *N. europaea* metabolism, but the higher Eu loadings inhibited ammonia oxidation; by 72 h the average ammonia oxidation activities relative to the no Eu control were 83.8±3.0% and 79.8±4.0%, respectively, for 50 and 100 ppm Eu. Effects on metabolism were also reflected in the measured pH values for the cultures. Ammonia oxidation by molecular oxygen is an acid producing reaction, as shown in equation 1, and in the cultures with active ammonia oxidation the pH dropped from the initial values ($\geq$ 7.5) to 6.0-6.5 by 48 h, and by 72 h the average pH of the 0 and 10 ppm Eu cultures was 6.1. Acidification also occurred in the 50 and 100 ppm cultures but more slowly. By 72 h, the 50 and 100 ppm Eu cultures had an average pH of ~6.5.

The effect of yttrium at 10 ppm was similar to that of Eu (i.e., negligible impact), but at 50 and 100 ppm the inhibitory effect of Y was comparatively much greater than Eu (Figure 1b). With the addition of 50 and 100 ppm Y, final nitrite production values were 34.1±4.1% and 21.4±0.8%, respectively, compared to the no Y control. The relative difference in impact between the two REE may reflect the greater molar amounts of Y exposed to the organisms compared to Eu; the lower atomic mass of Y compared to Eu results in equivalent masses of the elements corresponding to 70% greater Y than Eu in terms of moles. Again, the effect of the inhibition was manifested in the pH of the cultures; initial pH values of ≥7.5 dropped to ~6.1 by 72 hours in the 0 and 10 ppm Y cultures, but the pH remained unchanged in the 50 and 100 ppm cultures.

Effects of REEs on nitrite oxidation by **N. winogradskyi**. Activity of the *N. winogradskyi* cultures was monitored by measuring the disappearance of nitrite over time. Analogous to the case for *N. europaea*, no nitrifying activity was detected in the abiotic controls, and therefore those data are not presented in the figures or discussed further.

Compared to the *N. europaea, N. winogradskyi* appeared to be more sensitive to Eu (Figure 1c). Nitrite consumption was inhibited even at 10 ppm of Eu; by 72 hours, the relative nitrite consumption compared

to the no Eu control was 34.5±2.2%. The corresponding values for the 50 and 100 ppm Eu cultures were 29.3 ±8.1% and 17.2 ±1.4%, respectively.

Yttrium also had a deleterious effect on *N. winogradsky* (Figure 1d), and 10 ppm Y inhibited the cultures to a similar extent as the 10 ppm Eu; the relative nitrite consumption compared to the no Y control was 36.2±4.9%. As was observed for the *N. europaea*, the treatments receiving the 50 and 100 ppm amendments of Y were more inhibited than the corresponding treatments receiving Eu; relative nitrite consumption values were 4.3±0.9% and 2.8±1.2% for 50 ppm Y and 100 ppm Y, respectively.

Effects of TBP on nitrification activity

When provided to the *N. europaea* cultures, TBP and Isopar™ L alone appeared to inhibit nitrite production initially, but by 72 hours the cultures seemed to have almost completely "recovered." However, when TBP was added to the cultures already challenged with Eu, there appeared to be a synergistic effect--the inhibition by the metal was even greater (Figure 2a). In these cultures, inhibition of nitrification was also exhibited in the pH; at 72 h the average pH of the 10 ppm Eu + TBP cultures was ~6.5, and in the 50 and 100 ppm Eu cultures with TBP the final pH values remained at or above pH 7.5.

In contrast to the *N. europaea*, the *N. winogradsky* culture appeared to be extremely sensitive to TBP. In fact no nitrite consumption was observed in any of the cultures provided with 0.1 g/L TBP (Figure 2b). The effect appeared to be specific to TBP; when Isopar™ L alone was provided to the *N. winogradsky*, the cultures showed no inhibition compared to the controls with no added Y or organic extractants. This phenomenon is consistent with the thermodynamics of the system and the model predictions which show that TBP complexes the REEs and increases their aqueous solubility and presumably their availability to the cultures whilst the Isopar™ L (as a paraffin) does not lead to the same effect.

The mechanism of toxicity for TBP on the N. winogradskyi is unknown; previous studies have shown that TBP can be degraded by both pure and mixed cultures of microorganisms.[39-41]

Prediction and measurement of REE solubility in aqueous solution.

As mentioned earlier, the precipitation of REE hydroxides plays a key role in determining the availability of soluble REE species. While the actual concentration of REEs in a given system may be lower than the solubility of REE hydroxides due to the precipitation of other phases or adsorption phenomena, it is not likely to exceed it. Thus, the solubility of REE hydroxides provides a useful upper bound for the available REE concentration. Prior to applying the model to the actual media used in the experiments, we verified the accuracy of model predictions for the solubility of Eu and Y hydroxides. Details of this verification are given in the Supporting Information.

Upon satisfying ourselves that the model was acceptable for predicting Eu and Y solubility in simple aqueous solutions, we applied it to interpretation of the REE data from the experiments. In the *N. europaea* experiments (Sato medium), changes in the pH were expected to result in significant changes in the concentrations of soluble Eu and Y within the cultures. At the starting pH of the experiments (pH 7.5-8.0), with either Eu or Y, >98% of the REE added to any of the experimental treatments was expected to be insoluble (see Figures 3 and 4, solid lines). For Eu, at a starting pH of 7.5, the expected soluble

concentration was approximately 67 ppb for all 3 treatments (Figure 3). However, under the final pH conditions for the Eu amended cultures (pH ranging from 6.1 to 6.5), significantly more of the Eu was expected to be soluble. ICP-MS measurements did measure some soluble Eu in the 50 and 100 ppm treatments with pH < 7, but at concentrations of only 1-3 ppb, less than 1% of those expected. In the corresponding 50 and 100 ppm treatments where TBP was present, and the pH remained higher (>7.3), Eu remained below the detection limit (1 ppb) despite the higher predicted solubility in the presence of TBP (dashed lines in Figure 3). Figure 3 shows two clusters of measured data for Eu in the Sato medium. One cluster, which consists of data for samples which were abiotic and at pH 8.5-9.0 is consistent with the solubility of $Eu(OH)_3$, whereas the second cluster at lower pH values could be attributable to precipitation of a different mineral phase with a lower solubility than the hydroxides, namely a phosphate mineral phase ($EuPO_4$). The Sato medium contains 5 mM phosphate. The thermodynamic model predicted the solubility of the phosphate phase (dash-dotted lines in Figure 3) to be substantially lower than that of the hydroxide phases. The fact that the second cluster of data was located between the solubility curves of $Eu(OH)_3$ and $EuPO_4$ indicates the possibility that the observed concentrations reflect the slow, incomplete formation of a phosphate phase. The freshly precipitated phosphate phase may or may not have the same stoichiometry as the stable $EuPO_4$ phase. Identification of such a phase would require further experimental studies.

For the yttrium experiments with *N. europaea* (Sato medium), at pH 7.5 the soluble Y concentration was expected to be 147 ppb in all three Y-amended treatments. Based on the measured pH, significant soluble Y concentrations after 72 hours were expected in the 10 ppm Y cultures. However, a quantifiable level (>0.5 ppb) of soluble Y was only observed in one of the three replicates; the measured value was 9.7 ppb for a sample at pH 6.1. At that pH, all of the added Y was expected to be soluble (see solid curve in Figure 4). Again, in this case it appears likely that slow precipitation of a phosphate mineral is the cause of the low aqueous Y concentrations.

In the *N. winogradskyi* experiments (Soriano and Walker medium), unlike the case for ammonia oxidation, nitrite oxidation itself is not expected to alter the pH (equation 2). At 72 hours the pH of the *N. winogradskyi* cultures with Eu remained relatively unchanged from the time zero values of pH 7.5-8.0. In this pH range, aqueous Eu concentrations within the medium would be expected to be ≤45 ppb under all three Eu amendment conditions (Figure 5). For the 100 ppm Eu treatments, biotic and abiotic, the measured aqueous Eu values were between 21 and 43 ppb Eu, and for the treatments with 10 and 50 ppm Eu additions, the measured Eu was less than 10 ppb. These values were slightly lower than what was expected if Eu solubility was controlled by $Eu(OH)_3$, suggesting that in this system too another less soluble mineral phase may play a role. As in the Sato medium, a phosphate phase is a likely culprit; the Soriano and Walker medium contains phosphate at 0.6 mM. This is however much lower than the phosphate concentration (5 mM) in the Sato medium, and is reflected in the smaller discrepancy in the Soriano and Walker medium between measured Eu and Eu predicted based solely on $Eu(OH)_3$ solubility (solid lines in Figure 5); in other words the slow precipitation of an $EuPO_4$ mineral plays a smaller role in the Soriano and Walker medium compared to the Sato medium, for the given amounts of REE. This illustrates the fact that the formation of the hydroxide and phosphate phases is controlled by the amount of the phosphate available in the solution relative to the amount of the REE. If the total available amount of REE exceeds that of the phosphate, the phosphate ions will be predicted to precipitate almost completely as the REE phosphate phase (because of its extremely low solubility) and the remaining REE may form a hydroxide phase. In such an event, the REE concentration in the solution will be controlled by

the solubility of the REE hydroxide. This is illustrated in Figure 5 for the case where the total available Eu concentration is 100 ppm (0.66 mM), exceeding the total concentration of phosphate (0.6 mM) in the Soriano and Walker medium.

The impact of phosphate mineral formation in the Soriano and Walker medium was also observed in the experiments with *N. winogradskyi* and Y. Here too, measured Y concentrations appeared to be controlled largely by $Y(OH)_3$ solubility (Figure 6, solid lines). The predicted increased REE solubility in the presence of TBP (dashed lines) was supported by the limited data available; for example, in 50 ppm Y treatments that were both at pH 7.7, the measured aqueous concentrations for Y in the presence and absence of TBP were 156 and 83 ppb, respectively. Nevertheless, the suspected phosphate mineral precipitation had a much greater impact on Y solubility. The effect of the likely precipitation of a Y phosphate mineral was most obvious (larger deviation downward from the solid line) in the samples with the lowest amounts of added Y (10 ppm). However, kinetically delayed precipitation of a Y phosphate phase in the 50 and 100 ppm treatments was likely evidenced by an observed drop in pH to ≤ 7.3 for some of the 50 and 100 ppm treatments between the time zero measurement and 24 hours later. A decrease in pH would not be as evident for the 10 ppm Y case, where a smaller amount of Y phosphate could precipitate.

Another possible reason for the lower than expected (based on hydroxide mineral solubility) aqueous concentrations of both Eu and Y is that the REEs were adsorbed onto bacterial cell surfaces. Sorption of REEs on bacterial cells, even at low pH (i.e., pH less than 3), is well known. [42-45] However, even when samples of the Sato medium amended with 10 ppm Eu, in the absence of cells, were acidified to pH 6 the Eu was non-detectable (< 0.1 ppb), indicating that it was not available in solution to sorb to cells.

Implications

Our experimental results indicate that the presence of Eu and Y at levels above 10 ppm can inhibit ammonia oxidizing activity by *N. europaea*, even when initially most of the REE are expected to be insoluble. The nitrite oxidizing bacterium *N. winogradskyi* is more sensitive to Eu and Y; even the addition of 10 ppm Eu or Y caused more than 50% inhibition compared to the no REE controls. The soluble concentration of the REE did not appear to be the only determining factor with respect to inhibition; for instance, the addition of greater amounts of Eu or Y led greater inhibition, even when the changes in the aqueous concentrations of the REE were predicted to be negligible. The mechanism(s) by which insoluble Eu or Y could exert a toxic effect on the bacterial species is (are) unknown; an intriguing possibility is the formation of intracellular Eu or Y phosphate nanoparticles, which could promote reactions on their surfaces. , and will be the subject of future research.

Our findings also indicated that REE themselves may not be the only components of concern in a REE beneficiation or recycling wastewater with respect to acceptability at a municipal wastewater treatment plant. Organic compounds used for selective extraction of REE from aqueous process streams may also jeopardize biological treatment performance. The organic complexant TBP at 0.1 g/L, which is below its solubility limit in water (the concentration at which it would be expected to present following separation of organic and aqueous phases) appears to increase inhibition by the REEs. Indeed, with *N. winogradskyi*, no nitrifying activity at all was detected in the presence of TBP, whether the REE tested (Y) was present or not.

Future work will also include the examination of the impacts of Eu and Y and organic complexants (TBP and or other ligands) on microbial consortia from an operating wastewater treatment plant. It is possible that such consortia may be more resilient than the single species tested here, with respect to toxic effects of REE beneficiation or recycling wastewaters. Research in this area also contributes to our broader understanding of the behavior of REEs in ecosystems outside of wastewater treatment plants. With the rapid proliferation of REE -dependent products in the electronics and clean energy fields, unintended direct releases of REEs to the environment from industrial or mining operations as well as releases following disposal of REE-containing consumer products (e.g., landfill leachates) are almost certain to increase. Improved understanding of their behavior in the environment and effects on biotic systems are necessary to assess risk and to support the development of remediation methods if necessary.

SUPPORTING INFORMATION

A detailed description of the MSE thermodynamic model and associated modeling parameters are presented in the Supporting Information. This material is available free of charge via the Internet at http://pubs.acs.org.

AUTHOR INFORMATION

Corresponding Author

*Phone: 208-526-1242. Email: Yoshiko.fujita@inl.gov. Mail Stop: 83415-2203.

ACKNOWLEDGMENTS

We express our appreciation to D. LaCroix and J. Taylor at the University of Idaho/Center for Advanced Energy Studies for their assistance with ICP-MS measurements. We also thank M. Greenhalgh of INL for advice regarding wastewater composition and for provision of the organic extractants used in this study. This research is supported by the Critical Materials Institute, an Energy Innovation Hub funded by the U.S. Department of Energy, Office of Energy Efficiency and Renewable Energy, Advanced Manufacturing Office. The funding is provided via the DOE Idaho Operations Office Contract DE-AC07-05ID14517.

References

1. Binnemans, K.; Jones, P. T.; Blanpain, B.; Van Gerven, T.; Yang, Y. X.; Walton, A.; Buchert, M., Recycling of rare earths: a critical review. *J Clean Prod* **2013,** *51*, 1-22.
2. EPA, U. S. *Rare Earth Elements: A review of production, processing, recycling, and associated environmental issues*; 2012.
3. Merten, D.; Kothe, E.; Buechel, G., Studies on microbial heavy metal retention from uranium mine drainage water with special emphasis on rare earth elements. *Mine water and the environment* **2004,** *23*, 34-43.

4. Ngwenya, B. T.; Magennis, M.; Olive, V.; Mosselmans, J. F. W.; Ellam, R. M., Discrete Site Surface Complexation Constants for Lanthanide Adsorption to Bacteria As Determined by Experiments and Linear Free Energy Relationships. *Environ. Sci. Technol.* **2010,** *44*, (2), 650-656.
5. Ngwenya, B. T.; Mosselmans, J. F. W.; Magennis, M.; Atkinson, K. D.; Tourney, J.; Olive, V.; Ellam, R. M., Macroscopic and spectroscopic analysis of lanthanide adsorption to bacterial cells. *Geochim. Cosmochim. Acta* **2009,** *73*, (11), 3134-3147.
6. Texier, A. C.; Andres, Y.; Faur-Brasquet, C.; Le Cloirec, P., Fixed-bed study for lanthanide (La, Eu, Yb) ions removal from aqueous solutions by immobilized Pseudomonas aeruginosa: experimental data and modelization. *Chemosphere* **2002,** *47*, (3), 333-342.
7. Texier, A. C.; Andres, Y.; Le Cloirec, P., Selective biosorption of lanthanide (La, Eu, Yb) ions by Pseudomonas aeruginosa. *Environ. Sci. Technol.* **1999,** *33*, (3), 489-495.
8. Markai, S.; Andres, Y.; Montavon, G.; Grambow, B., Study of the interaction between europium (III) and Bacillus subtilis: fixation sites, biosorption modeling and reversibility. *J. Colloid Interface Sci.* **2003,** *262*, (2), 351-361.
9. Ozaki, T.; Suzuki, Y.; Nankawa, T.; Yoshida, T.; Ohnuki, T.; Kimura, T.; Francis, A. J., Interactions of rare earth elements with bacteria and organic ligands. *Journal of Alloys and Compounds* **2006,** *408*, 1334-1338.
10. Talbert, D.; Johnson, G., Some effects of rare earth elements and yttrium on microbial growth

Mycologia **1967,** *59*, 492–503.
11. Monafo, W. W.; Tandon, S. N.; Ayvazian, V. H.; Tuchschmidt, J.; Skinner, A. M.; Deitz, F., Cerium nitrate: a new topical antiseptic for extensive burns. *Surgery* **1976,** *80*, (4), 465-73.
12. Hu, X.; Ding, Z.; Chen, Y.; Wang, X.; Dai, L., Bioaccumulation of lanthanum and cerium and their effects on the growth of wheat (Triticum aestivum L.) seedlings. *Chemosphere* **2002,** *48*, (6), 621-629.
13. Chen, A.; Shi, Q.; Feng, J.; Ouyang, Y.; Chen, Y.; Tan, S., Dissociation of outer membrane for Escherichia coli cell caused by cerium nitrate. *Journal of Rare Earths* **2010,** *28*, (2), 312-315.
14. Chen, A.; Shi, Q.; Ouyang, Y.; Chen, Y., Effect of Ce3+ on membrane permeability of Escherichia coli cell. *Journal of Rare Earths* **2012,** *30*, (9), 947-951.
15. Peng, L.; Weiying, Z.; Xi, L.; Yi, L., Structural basis for the biological effects of Pr (III) ions: alteration of cell membrane permeability. *Biological trace element research* **2007,** *120*, (1-3), 141-147.
16. Peng, L.; Yi, L.; Zhexue, L.; Juncheng, Z.; Jiaxin, D.; Daiwen, P.; Ping, S.; Songsheng, Q., Study on biological effect of La< sup> 3+</sup> on< i> Escherichia coli</i> by atomic force microscopy. *Journal of inorganic biochemistry* **2004,** *98*, (1), 68-72.
17. Ren, S., Assessing wastewater toxicity to activated sludge: recent research and developments. *Environment International* **2004,** *30*, (8), 1151-1164.
18. Chandran, K.; Love, N. G., Physiological State, Growth Mode, and Oxidative Stress Play a Role in Cd(II)-Mediated Inhibition of Nitrosomonas europaea 19718. *Appl. Environ. Microbiol.* **2008,** *74*, (8), 2447-2453.
19. Lee, Y.-W.; Ong, S.-K.; Sato, C., Effects of heavy metals on nitrifying bacteria. *Water Sci. Technol.* **1997,** *36*, (12), 69-74.
20. Sato, C.; Schnoor, J. L.; McDonald, D. B., Characterization of effects of copper, cadmium and nickel on the growth of Nitrosomonas Europaea. *Environ. Toxicol. Chem.* **1986,** *5*, (4), 403-416.
21. Keener, W. K.; Arp, D. J., Kinetic Studies of Ammonia Monooxygenase Inhibition in Nitrosomonas europaea by Hydrocarbons and Halogenated Hydrocarbons in an Optimized Whole-Cell Assay. *Appl. Environ. Microbiol.* **1993,** *59*, (8), 2501-2510.
22. Kim, K. T.; Kim, I. S.; Hwang, S. H.; Kim, S. D., Estimating the combined effects of copper and phenol to nitrifying bacteria in wastewater treatment plants. *Water Res.* **2006,** *40*, (3), 561-568.

23. Grunditz, C.; Dalhammar, G., Development of nitrification inhibition assays using pure cultures of *Nitrosomonas* and *Nitrobacter*. *Water Res.* **2001,** *35*, (2), 433-440.
24. Grunditz, C.; Gumaelius, L.; Dalhammar, G., Comparison of inhibition assays using nitrogen removing bacteria: application to industrial wastewater. *Water Res.* **1998,** *32*, (10), 2995-3000.
25. Wang, S.; Gunsch, C. K., Effects of selected pharmaceutically active compounds on the ammonia oxidizing bacterium *Nitrosomonas europaea*. *Chemosphere* **2011,** *82*, (4), 565-572.
26. Tian, Q.; Liu, H., Densities and Viscosities of Binary Mixtures of Tributyl Phosphate with Hexane and Dodecane from (298.15 to 328.15) K. *Journal of Chemical & Engineering Data* **2007,** *52*, (3), 892-897.
27. Wang, P.; Anderko, A.; Springer, R. D.; Young, R. D., Modeling Phase Equilibria and Speciation in Mixed-Solvent Electrolyte Systems: II. Liquid-Liquid Equilibria and Properties of Associating Electrolyte Solutions. *Journal of Molecular Liquids* **2006,** *125*, (1), 37-44.
28. Wang, P.; Anderko, A.; Young, R. D., A Speciation-Based Model for Mixed-Solvent Electrolyte Systems. *Fluid Phase Equilibria* **2002,** *203*, (1-2), 141-176.
29. Sato, C.; Schnoor, J. L.; McDonald, D. B.; Huey, J., Test medium for the growth of *Nitrosomonas europaea*. *Appl. Environ. Microbiol.* **1985,** *49*, (5), 1101-1107.
30. Soriano, S.; Walker, N., The nitrifying bacteria in soils from Rothamsted classical fields and elsewhere. *Journal of Applied Bacteriology* **1973,** *36*, (3), 523-529.
31. Higgins, C. E.; Baldwin, W. H.; Soldano, B. A., Effects of Electrolytes and Temperature on the Solubility of Tributyl Phosphate in Water. *The Journal of Physical Chemistry* **1959,** *63*, (1), 113-118.
32. Painter, H. A.; Loveless, J. E., Effect of temperature and pH value on the growth-rate constants of nitrifying bacteria in the activated-sludge process. *Water Res.* **1983,** *17*, (3), 237-248.
33. APHA, *Standard methods for the examination of water and wastewater (1989) Washington*. American Public Health Association: 1989.
34. Hesford, E.; Mckay, H., The influence of diluent on extraction of europium and thorium nitrates by tri-n-butylphosphate. *Trans. Faraday Soc* **1958,** *45*, 537.
35. Gray, J. A.; Smutz, M., An equilibrium study of the chloride and nitrate systems of praseodymium and neodymium with tributyl phosphate and acid. *Journal of Inorganic and Nuclear Chemistry* **1966,** *28*, (9), 2015-2024.
36. Rosický, L.; Hála, J., Solvent extraction of yttrium (III) by TBP from acidic organic-aqueous solutions. *Journal of Radioanalytical and Nuclear Chemistry* **1983,** *80*, (1), 43-48.
37. Gray, P. R.; G., T. S., Extraction behavior of trivalent lanthanide and actinide elements into tributyl phosphate from hydrochloric and nitric acids. *U.S. Atomic Energy Commission Document* **1952,** *UCRL-2069*, 29.
38. Engel, M. S.; Alexander, M., Growth and autotrophic metabolism of *Nitrosomonas europaea*. *J. Bacteriol.* **1958,** *76*, (2), 217.
39. Rosenberg, A.; Alexander, M., Microbial Cleavage of Various Organophosphorus Insecticides. *Appl. Environ. Microbiol.* **1979,** *37*, (5), 886-891.
40. Thomas, R. A. P.; Morby, A. P.; Macaskie, L. E., The biodegradation of tributyl phosphate by naturally occurring microbial isolates. *FEMS Microbiol. Lett.* **1997,** *155*, (2), 155-159.
41. Thomas, R. A. P.; Macaskie, L. E., The effect of growth conditions on the biodegradation of tributyl phosphate and potential for the remediation of acid mine drainage waters by a naturally-occurring mixed microbial culture. *Applied Microbiology and Biotechnology* **1998,** *49*, (2), 202-209.
42. Andrès, Y.; Texier, A. C.; Le Cloirec, P., Rare earth elements removal by microbial biosorption: A review. *Environmental Technology* **2003,** *24*, (11), 1367-1375.
43. Takahashi, Y.; Chatellier, X.; Hattori, K. H.; Kato, K.; Fortin, D., Adsorption of rare earth elements onto bacterial cell walls and its implication for REE sorption onto natural microbial mats. *Chem. Geol.* **2005,** *219*, (1-4), 53-67.

44. Tsuruta, T., Accumulation of rare earth elements in various microorganisms. *Journal of Rare Earths* **2007,** *25*, (5), 526-532.
45. Yoshida, T.; Ozaki, T.; Ohnuki, T.; Francis, A. J., Adsorption of rare earth elements by gamma-Al2O3 and Pseudomonas fluorescens cells in the presence of desferrioxamine B: implication of siderophores for the Ce anomaly. *Chem. Geol.* **2004,** *212*, (3-4), 239-246.
46. Akselrud, N.; Ermolenko, V., Hydroxides and basic chlorides of europium, terbium and holmium. *Russ. J. Inorg. Chem* **1961,** *6*, 397-399.
47. Bernkopf, M. F. Technische Universität München, 1984.
48. Smith, R.; Martell, A., Critical Stability Constants, 4Plenum. *New York* **1976**, 75.
49. Spivakovskii, V.; Moisa, L., Composition, activity products, and free energies of formation of scandium, yttrium, lanthanum, and lanthanide hydroxide chlorides and hydroxides. *Russian Journal of Inorganic Chemistry* **1977,** *22*, (5), 643-645.
50. Davis Jr, W.; Mrochek, J.; Hardy, C., The system: Tri-n-butyl phosphate (TBP)-nitric acid-water—I activities of TBP in equilibrium with aqueous nitric acid and partial molar volumes of the three components in the TBP phase. *Journal of Inorganic and Nuclear Chemistry* **1966,** *28*, (9), 2001-2014.
51. Kertes, A., Solute-solvent interaction in the system hydrochloric acid-water-tri-n-butyl phosphate. *Journal of Inorganic and Nuclear Chemistry* **1960,** *14*, (1), 104-113.
52. Kertes, A.; Kertes, V., Solvent extraction of mineral acids. IV. Solute-solvent interaction in the system perchloric acid-water-tri-N-butyl phosphate. *Journal of Applied Chemistry* **1960,** *10*, (7), 287-292.
53. Scargill, D.; Alcock, K.; Fletcher, J.; Hesford, E.; McKay, H., Tri-n-butyl phosphate as an extracting solvent for inorganic nitrates—II Yttrium and the lower lanthanide nitrates. *Journal of Inorganic and Nuclear Chemistry* **1957,** *4*, (5), 304-314.
54. Siekierski, S., Extraction from solutions of perchloric acid by tributylphosphate—I: Partition coefficients for zirconium, thorium, cerium, promethium and yttrium. *Journal of Inorganic and Nuclear Chemistry* **1959,** *12*, (1), 129-135.

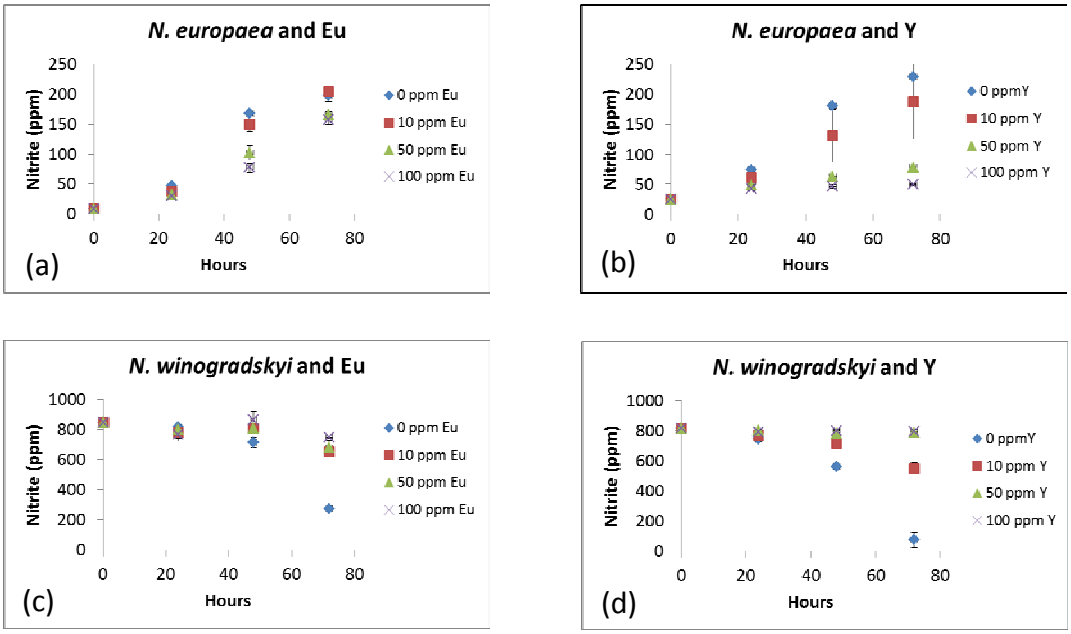

Figure 1. Nitrification activity for *Nitrosomonas europaea* and *Nitrobacter winogradskyi* in the presence of europium and yttrium. (a) Nitrite production by *N. europaea* in presence of Eu. (b) Nitrite production by *N. europaea* in presence of Y. (c) Nitrite consumption by *N. winogradskyi* in presence of Eu. (d) Nitrite consumption by *N. winogradskyi* in presence of Y. Error bars represent one standard deviation.

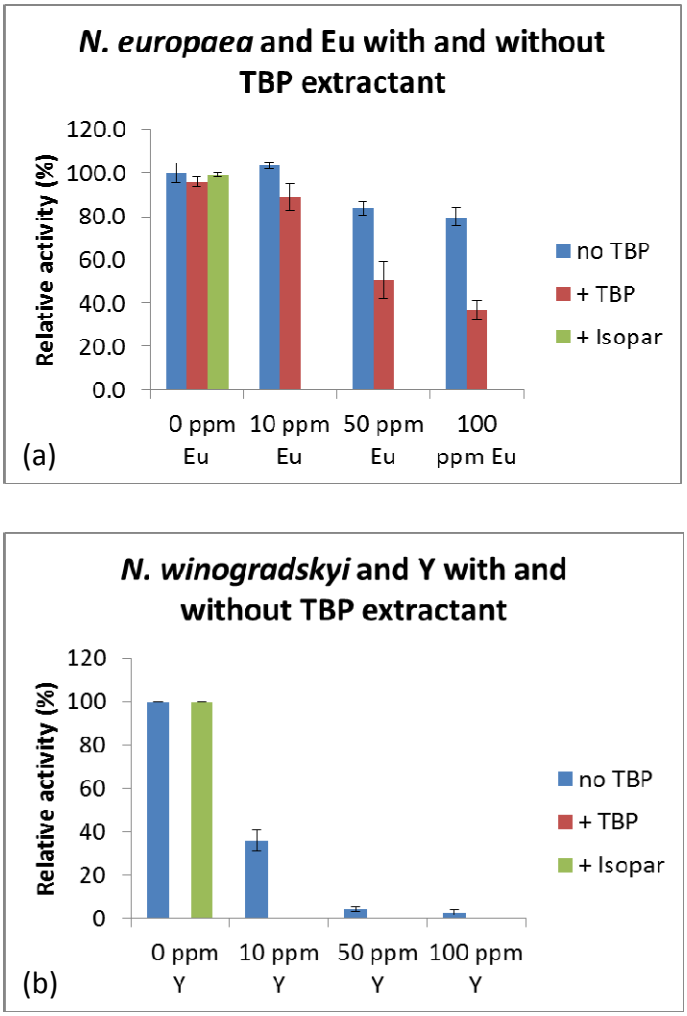

Figure 2. Effect of organic extractants on nitrification activity by *Nitrosomonas europaea* and *Nitrobacter winogradskyi*. (a) Relative activity compared to no Eu, no TBP control for *N. europaea*. (b) Relative activity compared to no Y, no TBP control for *N. winogradskyi*. Error bars represent one standard deviation.

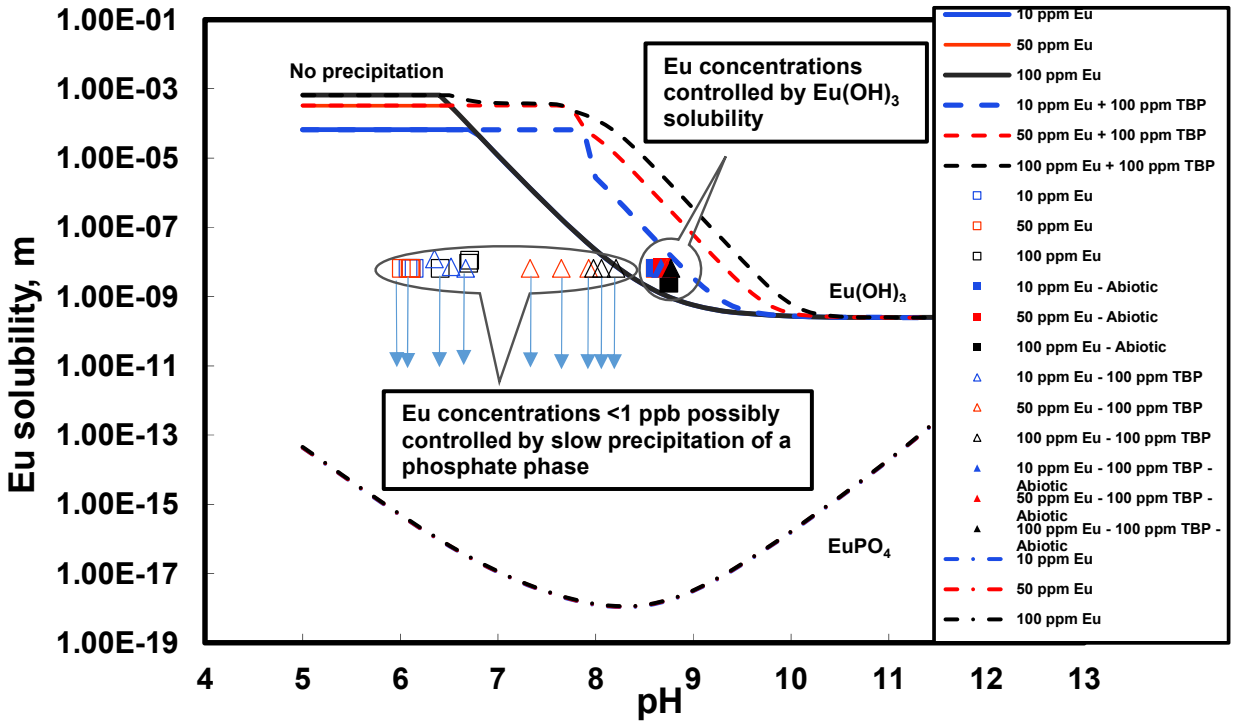

Figure 3. Predicted solubility of europium in the Sato et al. [29] medium in the presence or absence of TBP compared to the measured concentrations as a function of pH. Symbols and curves represent experimental and predicted solubility values, respectively. Downward arrows on the symbols indicate that the values plotted are actually the detection limits; actual values for the samples were at or below these levels. The solid curves show the solubility when only $Eu(OH)_3$ precipitates. The dash-dotted curves (which coincide with each other) represent the solubility when both $Eu(OH)_3$ and crystalline $EuPO_4$ can precipitate.

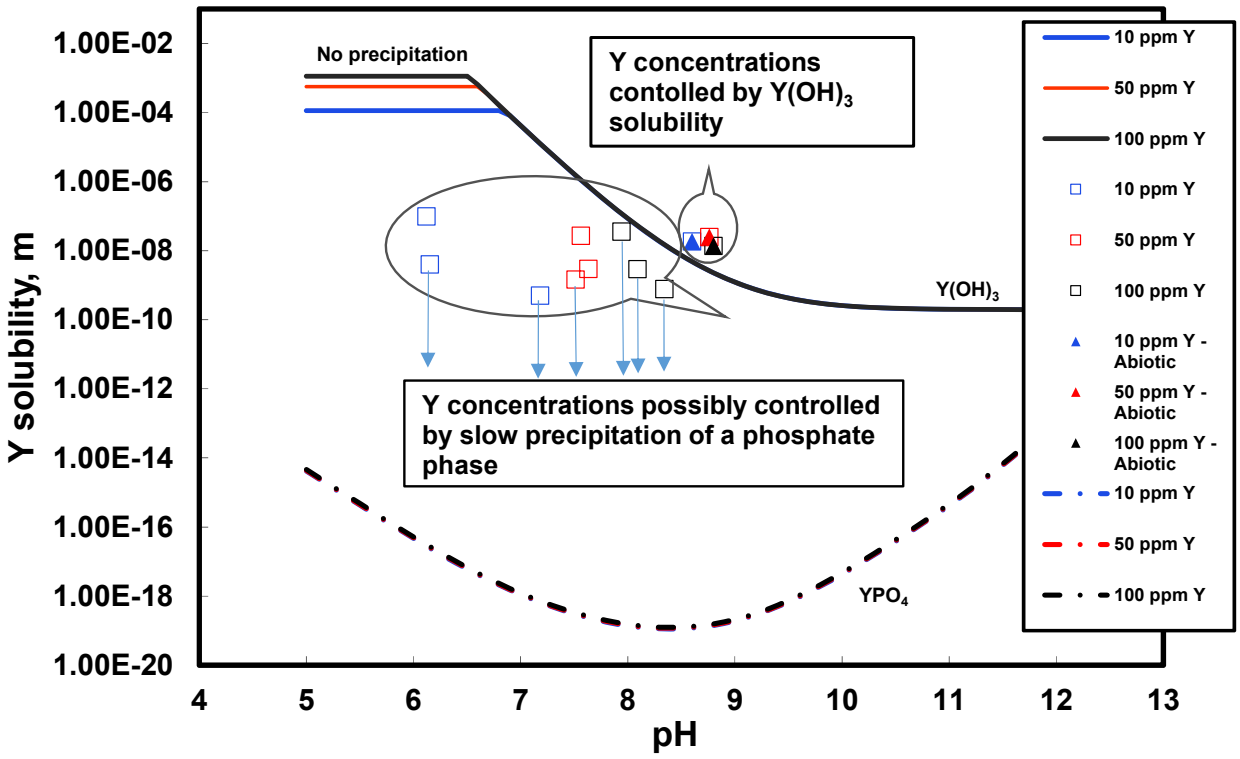

Figure 4. Predicted solubility of yttrium in the Sato et al. [29] medium compared to the measured data as a function of pH. Symbols and curves represent experimental and predicted solubility values, respectively. Downward arrows on the symbols indicate that the values plotted are actually the detection limits; actual values for the samples were at or below these levels.

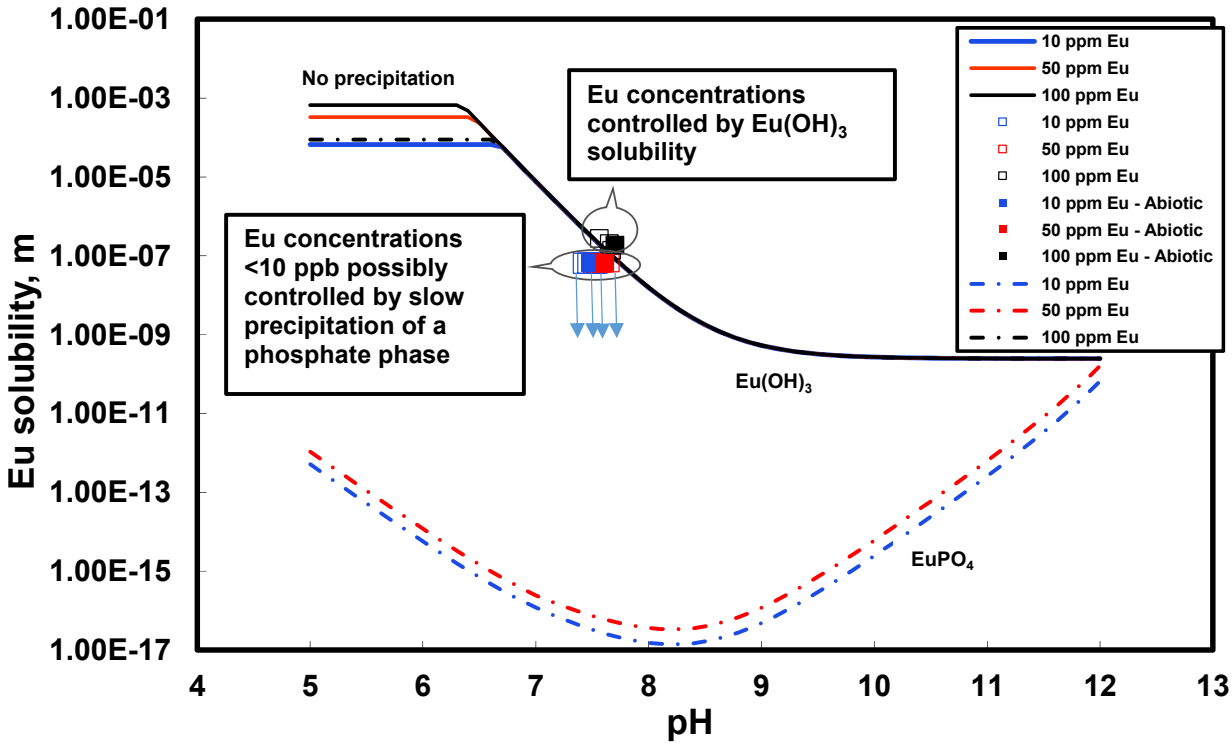

Figure 5. Comparison of the predicted solubility of europium in the Soriano and Walker[30] medium with the measured concentrations as a function of pH. Symbols and curves represent experimental and predicted solubility values, respectively. Downward arrows on the symbols indicate that the values plotted are actually the detection limits; actual values for the samples were at or below these levels. The solid curves show the solubility when only $Eu(OH)_3$ precipitates. The dash-dotted curves represent the solubility when both $Eu(OH)_3$ and crystalline $EuPO_4$ can precipitate (note that at 100 ppm Eu the solubility is controlled by $Eu(OH)_3$ because $Eu(OH)_3$ precipitation follows a practically complete precipitation of phosphates in the form of $EuPO_4$).

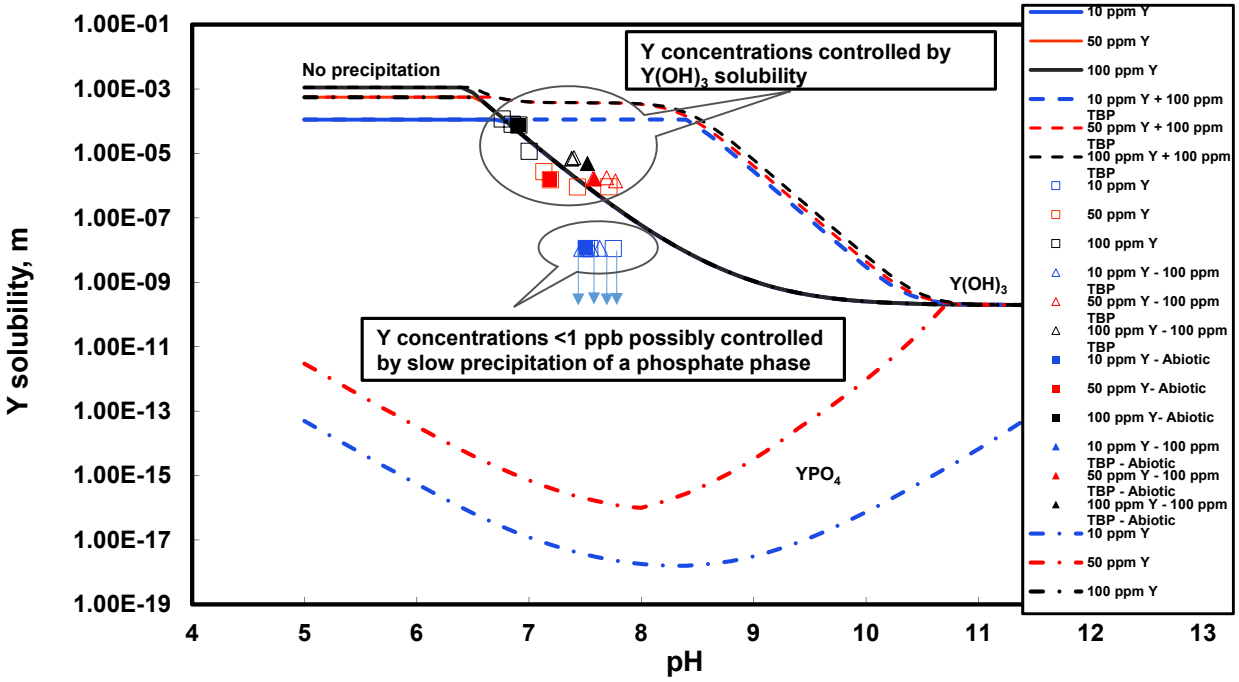

Figure 6. Predicted solubility of yttrium in Soriano and Walker[30] medium in the presence or absence of TBP compared to the measured data as a function of pH. Symbols and curves represent experimental and predicted solubility values, respectively. Downward arrows on the symbols indicate that the values plotted are actually the detection limits; actual values for the samples were at or below these levels.

Table 1. Sources of the experimental data used to determine the thermodynamic model parameters.

System	Data type	Temperature, °C	Pressure, atm	REE distribution coefficient range	Reference
$Eu(OH)_3$-H_2O	K_{sp}^{*}	25	1	-	[46-48]
$Eu(OH)_3$-H_2O-$NaClO_4$	K_{sp} & K'_{sp}*	25	1	-	[47]
$Eu(OH)_3$-H_2O-NaCl-NaOH	K_{sp}	25	1	-	[46, 48]
$Y(OH)_3$-H_2O-NaCl	K_{sp}^{**}	25	1	-	[49]
TBP-HNO_3-H_2O	LLE	25	1	-	[50]
TBP-HCl-H_2O	LLE	20	1	-	[51]
TBP-$HClO_4$-H_2O	LLE	27	1	-	[52]
TBP-HNO_3-H_2O-Eu	LLE-REE distribution	25	1	0.105-64	[53]
TBP-HNO_3-H_2O-Y	LLE-REE distribution	25	1	0.044-220	[53]
TBP-$HClO_4$-H_2O-Y	LLE-REE distribution	25	1	0.039-130	[54]
TBP-HCl-H_2O-Y	LLE-REE distribution	25	1	0.004-19.113	Estimated§
TBP-HCl-H_2O-Eu	LLE-REE distribution	25	1	0.0043-2.5976	[37] + Estimated

* Solubility product: $K'sp = [Eu^{3+}][OH^-]^3$; $Ksp = (K'sp)\gamma_{Eu^{3+}}(\gamma_{OH^-})^3$

** Solubility product: $Ksp = (K'sp)\gamma_{Y^{3+}}(\gamma_{OH^-})^3$

§ Data generated using the procedure explained in the text

Supporting Information

Effects of simulated rare earth recycling wastewaters on biological nitrification

Yoshiko Fujita, Joni Barnes, Ali Eslamimanesh, Malgorzata M. Lencka, Andrzej Anderko, Richard E. Riman, and Alexandra Navrotsky

Mixed-Solvent Electrolyte (MSE) Thermodynamic Model

The Mixed-Solvent Electrolyte (MSE) model combines formulations for reproducing the standard-state properties of individual species and the excess Gibbs energy (and, hence, the activity coefficients) in multicomponent mixtures. The combined framework was described in detail in previous papers.[1-3] Here, we briefly outline the model in order to explain and document the parameters that have been developed in this study.

To take into account the various intermolecular and electrostatic forces in an electrolyte solution, the expression for the excess Gibbs energy is expressed as follows:

$$G^{\mathrm{ex}} = G^{\mathrm{ex}}_{\mathrm{LR}} + G^{\mathrm{ex}}_{\mathrm{II}} + G^{\mathrm{ex}}_{\mathrm{SR}} \tag{S1}$$

where $G^{\mathrm{ex}}_{\mathrm{LR}}$ denotes the contribution of long-range electrostatic interactions, $G^{\mathrm{ex}}_{\mathrm{II}}$ accounts for ionic (ion-ion and ion-molecule) interactions, and $G^{\mathrm{ex}}_{\mathrm{SR}}$ stands for the short-range contributions resulting from intermolecular interactions. The long-range interaction contribution is calculated from the Debye-Hückel theory as revised by Pitzer[4] (expressed in terms of mole fractions). The ion-interaction contribution is explained by an ionic strength-dependent, symmetrical virial -type expression:[2]

$$\frac{G^{\mathrm{ex}}_{\mathrm{II}}}{RT} = -\left(\sum_i n_i\right)\sum_i\sum_j x_i x_j B_{ij}(I_x) \tag{S2}$$

Where $B_{ij}(I_x) = B_{ji}(I_x)$, $B_{ii} = B_{jj} = 0$ and the ionic strength dependence of B_{ij} is expressed by:

$$B_{ij}(I_x) = b_{ij} + c_{ij}\exp(-\sqrt{I_x + a_1}) \tag{S3}$$

where b_{ij} and c_{ij} are binary interaction parameters and a_1 has a fixed value of 0.01. The parameters b_{ij} and c_{ij} are obtained by regressing experimental data and are generally calculated as functions of temperature and pressure as follows:

$$b_{ij} = b_{0,ij} + b_{1,ij}T + b_{2,ij}/T + b_{3,ij}T^2 + b_{5,ij}\exp(b_{6,ij}T) + b_{7,ij}T\ln T + b_{8,ij}/\exp(b_{9,ij}T) + b_{0p,ij}P + (b_{2p,ij}/T)P \tag{S4}$$

$$c_{ij} = c_{0,ij} + c_{1,ij}T + c_{2,ij}/T + c_{3,ij}T^2 + c_{5,ij}\exp(c_{6,ij}T) + c_{7,ij}T\ln T + c_{8,ij}/\exp(c_{9,ij}T) \tag{S5}$$

For the vast majority of species pairs *i-j*, no more than the first three coefficients are required in the eqs. S4-S5.

The short-range interaction contribution is obtained from the UNIQUAC model:[5]

$$\frac{G_{SR}^{ex}}{RT} = \left(\sum_{\mathrm{i}} \mathrm{n_i}\right)\left[\sum_{\mathrm{i}} x_i \ln\frac{\phi_i}{x_i} + \frac{Z}{2}\sum_i q_i x_i \ln\frac{\theta_i}{\phi_i}\right] - \left(\sum_{\mathrm{i}} \mathrm{n_i}\right)\left[\sum_{\mathrm{i}} q_i x_i \ln\left(\sum_j \theta_j \tau_{ij}\right)\right] \tag{S6}$$

In Eq. (S6),

$$\theta_i = \frac{q_i x_i}{\sum_j q_j x_j} \tag{S7}$$

$$\phi_i = \frac{r_i x_i}{\sum_j r_j x_j} \tag{S8}$$

$$\tau_{ji} = \exp\left(-\frac{a_{ji}}{RT}\right) \tag{S9}$$

where q_i and r_i are the surface and size parameters, respectively, Z is a fixed coordination number ($Z = 10$), and a_{ij} ($a_{ij} \neq a_{ji}$) is the binary interaction parameter expressed as follows:

$$a_{ij} = a_{ij}^{(0)} + a_{ij}^{(1)}T + a_{ij}^{(2)}T^2 + (a_{ij}^{(P0)} + a_{ij}^{(P1)}T + a_{ij}^{(P2)}T^2)P \tag{S10}$$

A small subset of the coefficients of Eq. S10 is sufficient for most of species pairs of interest. For systems containing only strong electrolytes, only the ion interaction parameters (Eqs. S4 and S5) are needed. Interactions involving neutral species are represented by short-term parameters (Eq. S10).

The activity coefficients are calculated from Eq. S1 by differentiation with respect to the number of moles.[6] These activity coefficients are symmetrically normalized (they are unity for each pure component). They are later converted to unsymmetrical normalization, in which the activity coefficient of the solvent (water) is equal to 1 for a pure solvent and those of all the remaining species approach 1 at infinite dilution.[2]

Liquid-liquid equilibria are computed by solving the equations that express the equality of chemical potentials of species *i* in the two coexisting liquid phases (L1 and L2) as follows:

$$\mu_i^{L1} = \mu_i^{L2} \tag{S11}$$

in which μ_i^L is the chemical potential of species *i* in the liquid phase and superscripts 1 and 2 refer to the first and the second liquid phases, respectively.

In the MSE framework,[1, 2] the chemical potential of a species *i* in a liquid phase is calculated by:

$$\mu_i^L = \mu_i^{L,0,m}(T,P) + RT\ln\frac{1000}{M_{H_2O}} + RT\ln x_i\gamma_i^{x,*}(T,P,\mathbf{x}) \quad \text{(S12)}$$

where $\mu_i^{L,0,m}(T,P)$ represents the molality-based standard-state chemical potential, x_i is the mole fraction, and $\gamma_i^{x,*}(T,P,\mathbf{x})$ stands for the unsymmetrically normalized, mole fraction-based activity coefficient (calculated from Eq. S1 as previously described) and M_{H_2O} is the molecular weight of water. The standard-state chemical potential is calculated as a function of temperature and pressure from the Helgeson-Kirkham-Flowers (HKF) equation of state.[7-11] The Haar-Gallagher-Kell equation of state[12] is applied to calculate the the standard-state chemical potential of pure water.

For speciation calculations, the chemical effects due to the formation of ion pairs and complexes are explicitly considered using chemical equilibria.[3] Furthermore, the same chemical equilibrium formalism is employed for solid–liquid equilibria (SLE) computation.[3] The standard-state chemical potentials μ_i^0 are to be calculated for all species together with the activity coefficients. For solids, these values are evaluated using the reference-state Gibbs energy of formation, entropy and heat capacity according to standard thermodynamic relationships.[3]

Acid-base equilibria are simulated on the assumption that protons are solvated (e.g., in the form of hydronium ions in aqueous environments). A methodology for calculating pH in systems with solvated protons has been described by Kosinski et al.[13]

Methodology to determine the required thermodynamic model parameters for REE-TBP complexes

1. It has been assumed that TBP forms the $REE(NO_3)_3TBP$, $REE(ClO_4)_3TBP$, and $REECl_3TBP$ complexes in the REEs extraction systems from HNO_3, $HClO_4$ and HCl aqueous solutions through the following reactions:

$$Y^{3+} + 3NO_3^- + TBP \rightarrow Y(NO_3)_3TBP \quad \text{(S13)}$$

$$Y^{3+} + 3ClO_4^- + TBP \rightarrow Y(ClO_4)_3TBP \quad \text{(S14)}$$

$$Y^{3+} + 3Cl^- + TBP \rightarrow Y(Cl)_3TBP \quad \text{(S15)}$$

$$Eu^{3+} + 3NO_3^- + TBP \rightarrow Eu(NO_3)_3TBP \quad \text{(S16)}$$

$$Eu^{3+} + 3Cl^- + TBP \rightarrow Eu(Cl)_3TBP \quad \text{(S17)}$$

2. The required model parameters have been obtained to represent the distribution of Y between the HNO_3 and $HClO_4$–containing aqueous phases and the TBP organic phase and the distribution of Eu between the HNO_3–containing aqueous phase and the TBP organic phase.
3. Two sets of pseudo-experimental data have been generated for the distribution of Y/Eu between the HCl aqueous phase and the TBP organic phase using the available data point for Eu

distribution in this system (see Table 2) and the similarity in the behavior of REEs in various TBP extraction systems.

4. The reference-state Gibbs energies of formation of $Eu(NO_3)_3TBP$ and $Y(NO_3)_3TBP$ have been determined as model parameters by regressing the relevant experimental data. Then, it has been assumed that the Gibbs energy values for reactions S13-S15 and those for reactions S16 and S17 are equal, respectively. Using the value of the Gibbs energy of reaction S13, the reference-state Gibbs energy of formation of $Y(ClO_4)_3TBP$ has been calculated, making sure that the latter assumption results in a reasonable representation of the Y distribution data.[14]
5. Analogous computations have been made to obtain the reference-state Gibbs energy of formation of YCl_3TBP and $EuCl_3TBP$. Then, the required interaction parameters of the model have been determined to represent the Y/Eu distribution between the HCl aqueous phase and TBP organic phase.

Determination of the required thermodynamic model parameters to account for solubility of $Eu(OH)_3$ and $Y(OH)_3$

Although the solubility of REE hydroxides in aqueous solutions has been studied in the literature, the amount of available data varies widely for various REEs. Specifically, sparse data exist for Eu and Y compared to for example Nd. The solubility of REE hydroxides generally follows the relative basicity order as established by Levy[15] (see also Endres[16] and Moeller and Kremers[17]):

La>Ce(III)>Pr>Nd>Y>Eu>Gd>Sm>Tb>Dy>Ho>Er>Tm>Yb>Lu>Sc>Ce(IV)

Figure S1 depicts the solubilities of $Nd(OH)_3$, $Y(OH)_3$, and $Eu(OH)_3$ in aqueous solutions calculated using the MSE thermodynamic framework. The model represents the solubility data for $Nd(OH)_3$ within their experimental scattering. Although no comparable data exist for Eu and Y, the model accurately represents the available K_{sp} values for all three elements, in a quantitative agreement with the above basicity order. Furthermore, the pH dependence of the solubilities is determined by the standard-state properties of the hydrolyzed forms of rare earth metals, which have been evaluated by Shock and Helgeson,[18] Shock et al.[19, 20] and Haas and coworkers.[21] Thus, the model provides a good estimate of the solubility of $Eu(OH)_3$ and $Y(OH)_3$ as well as an accurate representation of solubility data for $Nd(OH)_3$. The results shown in Figure S1 confirm the relative basicity order of Nd>Y>Eu as reported by Levy.[15]

Table S1. Parameters to determine the properties of individual species: standard partial molar Gibbs energy of formation, entropy, and parameters of the Helgeson-Kirkham-Flowers equation of state[7-11] for standard partial molar thermodynamic properties ($a_{\mathrm{HKF},1,..4}$, $c_{\mathrm{HKF},1}$, $c_{\mathrm{HKF},2}$, ω).

Species	$\Delta\overline{G}_f^0$	$\overline{S}^0$	$a_{HKF,1}$	$a_{HKF,2}$	$a_{HKF,3}$	$a_{HKF,4}$	$c_{HKF,1}$	$c_{HKF,2}$	ω
	kcal.mol^{-1}	cal.mol^{-1}K^{-1}	cal.mol^{-1}.bar^{-1}	cal.mol^{-1}	cal.K.mol^{-1}.bar^{-1}	cal.K.mol^{-1}	cal.mol^{-1}K^{-1}	cal.K.mol^{-1}	cal.mol^{-1}
Na^+ (1)	-62.59106	13.95999	0.1839	-228.5	3.256	-27260	18.18	-29810	33060
Ca^{2+} (1)	-132.12	-13.5	-0.01947	-725.2	5.2966	-24792	9	-25220	123660
Fe^{2+} (1)	-21.87	-25.3	-0.07867	-969.69	9.5479	-23780	14.786	-46437	143820
Mg^{2+} (1)	-108.499	-33.00669	-0.08217	-859.9	8.39	-23900	20.8	-58920	153720
OH^- (1)	-37.59512	-2.55999	0.12527	7.38	1.8423	-27821	4.15	-103460	172460
H_3O^+ (2)	-56.68619	16.7289	0.451232	-21.2711	-8.64735	20487	14.6773	16975.9	-13672.5
Cl^- (1)	-31.37906	13.55999	0.4032	480.1	5.563	-28470	-4.4	-57140	145600
ClO_4^- (1)	-2.04000	43.5	0.81411	1556.54	-7.8077	-34224	16.45	-65700	96990
NO_3^- (1)	-26.50693	35.12	0.73161	678.24	-4.6838	-30594	7.7	-67250	109770
SO_4^{2-} (1)	-177.93	4.5	0.83014	-198.46	-6.2122	-26970	1.64	-179980	314630
PO_4^{3-} (1)	-243.499	-305.3011	-0.05258	-905.76	9.2927	-24045	-15.1599	-284155	561140
HCl (aq) *,(1)	-20.8937	40.4935	1.0217	0	0	0	16.1429	1.00E-06	1.00E-06
NaOH (aq) (1)	-91.99163	39.37519	1.43137	0	0	0	0	0	0
HNO_3 (aq) (1)	-24.82457	31.75189	0	0	0	0	22.2097	1.00E-06	1.00E-06
TBP (aq) (3)	-194.2794	56.08848	6.60318	0	0	0	480.3799	-1070730	1.00E-06
Y^{3+} (1)	-163.8	-60	-0.20463	-1277.41	10.7611	-22508	21.5366	-56622	248900
YO_2H (aq) (1)	-241.7	31.8	0.44506	308.28	4.5443	-29063	-50.6646	-226916	-30000
YOH^{+2} (1)	-210	-17.2	0.24985	-168.06	6.4099	-27094	8.0136	-66196	132010
YO^{+1} (1)	-198.1	-2.2	0.25778	-148.9	6.3393	-27173	-22.6289	-149102	58310
YCl_3TBP (aq) (3)	-473.9037	36.8	0	0	0	0	0	0	0
$Y(ClO_4)_3$TBP (aq) (3)	-376.446	126	0	0	0	0	0	0	0
$Y(NO_3)_3$TBP (aq) (3)	-459.2873	101	0	0	0	0	0	0	0
Eu^{3+} (1)	-137.3	-53	-0.31037	-1536	11.787	-21440	6.0548	-104900	231610
EuO_2H (aq) (1)	-216	42.4	0.48064	395.4	4.1968	-29424	-64.906	-276415	-3000
$EuOH^{+2}$ (1)	-183.2003	-7.999522	0.26569	-129.69	6.2659	-27253	0.5828	-87585	118150
EuO^{+1} (1)	-171.7	7.7	0.27458	-107.43	6.1663	-27345	-30.6415	-172120	43220
$EuCl_3$TBP (aq) (3)	-449.4199	44	0	0	0	0	0	0	0

$Eu(NO_3)_3TBP$ (aq) [3]	-434.8038	108	0	0	0	0	0	0	0

* aq: aqueous; § Not applicable

[1] Parameters from[18-20, 22]

[2] Parameters from previous work[1]

[3] Parameters regressed in this study

Table S2. Gibbs energy of formation, entropy and heat capacity coefficients for solid phases.

Solid phase	$\Delta_f G^o$	S^o	Cp (cal·mol^{-1}·K^{-1}) = A + BT + C/T^2 + DT^2 + ET^3				
	kcal·mol^{-1}	cal·mol^{-1}·K^{-1}	*A*	*B*	*C*	*D*	*E*
$Eu(OH)_3$	-286.1405	33	-1.490679	0.100406	0	0.000311	-9.56E-07
$Y(OH)_3$	-311.9596	27	26.20846	0	0	0	0
$EuPO_4$	-415.9677	21.31881	32.87763	0.0042288	-665727	0	0
YPO_4	-443.886	26	24.8	0	0	0	0

Table S3. Binary parameters used in the ionic-interaction term (Eqs. S4 and S5)

Species *i*	Species *j*	$b_{0,ij}$	$b_{1,ij}$	$b_{2,ij}$	$b_{3,ij}$	$c_{0,ij}$	$c_{1,ij}$	$c_{2,ij}$	$c_{3,ij}$	Source
HCl (aq)	H_2O	1.19159	0	-908.555	0	0	0	0	0	*
HNO_3 (aq)	H_2O	-3.22864	0	0	0	0	0	0	0	*
HCl (aq)	H_3O^+	0	0	-1922.21	0	0	0	0	0	*
HCl (aq)	Cl^-	0	0	-1922.21	0	0	0	0	0	*
HNO_3 (aq)	H_3O^+	1.54804	0	-1081.11	0	0	0	0	0	*
HNO_3 (aq)	NO_3^-	1.54804	0	-1081.11	0	0	0	0	0	*
HNO_3 (aq)	C^{l-}	-34.1171	0	8600.59	0	0	0	0	0	*
OH^-	NO_3^-	-18.19633	2.43e-02	8014	0	-38.54484	6.11e-02	866.9075	0	*
OH^-	Cl^-	26.7086	-2057.68	0	0	-47.8708	7916.05	0	0	*
ClO_4^-	H_3O^+	23.8793	0	-20460.4	0	-45.5671	0	29406.3	0	*
NO_3^-	H_3O^+	3.2113	0	-2127.87	0	0	0	0	0	*
Cl^-	H_3O^+	75.511	-8.59e-02	-21132.3	0	-167.683	0.228176	35827.5	0	*
NO_3^-	Cl-	15.1696	0	-5.06E+03		-21.0094	0	7500.53	0	*
Na^+	Cl^-	-213.999	1.86323	16036.8	0	202.887	-2.15391	-9832.11	0	*
Ca^{2+}	Cl^-	-95.9932	0.470226	-17370.9	-5.68e-04	-0.694366	-0.421581	43725.9	0.000791 11	*
Na^+	Ca^{2+}	11.2685	-0.0263793	2905.5	0	0	0	-6685.21	0	*
Mg^{2+}	Na^+	-28.8624	0.0351923	8744.27	0	0	0	-6373.88	0	*
NaOH (aq)	H_2O	13.1682	-1.25e-02	-2316.81	0	0	0	0	0	*
NaOH (aq)	Cl^-	-1.72916	0	2454.07	0	0	0	0	0	*
OH^-	Na^+	-223.724	2.86773	568.553	0	455.366	-5.72606	-14362.3	0	*
ClO_4^-	Na^+	126.029	-0.180524	-25481.6	0	-273.004	0.381704	53315.8		*
Na^+	H_3O^+	-7.5758	0	6221.7	0	4.61757	0	-8146.65	0	*
TBP (aq)	ClO_4^-	-24.94993	0	-7488.722	0	47.02546	0	0	0	**
TBP (aq)	H_3O^+	16.03884	0	-246.1059	0	8.374334	0	0	0	**
TBP (aq)	NO_3^-	19.79256	0	-3139.597	0	-32.74986	0	0	0	**
TBP (aq)	Cl^-	-4.84907	0	-1769.626	0	-18.14084	0	0	0	**
$Y(ClO_4)_3$TBP (aq)	H_3O^+	-29.32529	0	0	0	0	0	0	0	**

$Y(NO_3)_3TBP$ (aq)	H_3O^+	1302.19	0	0	0	-64.87495	0	0	0	**
$Y(NO_3)_3TBP$ (aq)	NO_3^-	-1252.264	0	0	0	0	0	0	0	**
YCl_3TBP (aq)	H_3O^+	-16.60342	-5.57e-02	0	0	95.76106	0.3211842	0	0	**
YCl_3TBP (aq)	Cl^-	-153.2699	0	0	0	0	0	0	0	**
$EuCl_3TBP$ (aq)	H_3O^+	20.6274	0	0	0	-13.2312	-4.41e-02	0	0	**
$Eu(NO_3)_3TBP$ (aq)	H_3O^+	11.79634	0	0	0	0	0	0	0	**
Eu^{3+}	H_3O^+	-6.947305	0	0	0	0	0	0	0	**
Eu^{3+}	Cl^-	-36.82582	-7.75E-02	-915.3253	0	-57.81919	0.5073278	0	0	**
Y^{3+}	Cl^-	-878.9536	1.133835	140975.1	0	1565.57	-1.862954	-271790.1	0	**

Species *i*	Species *j*	$b_{5,ij}$	$b_{6,ij}$	$b_{7,ij}$	$b_{8,ij}$	$b_{9,ij}$	$b_{P0,ij}$	$b_{P2,ij}$	Source
Na^+	Cl^-	-3.13e-05	0.0221142	-0.244873	-4963540	0.0519778	0.00689898	-2.156	*
OH^-	Na^+	-1.20074e-06	2.65863e-02	-0.397426	-73972	3.39350e-02	0	-1.13802	*

Species *i*	Species *j*	$c_{5,ij}$	$c_{6,ij}$	$c_{7,ij}$	$c_{8,ij}$	$c_{9,ij}$	*Source*
Na^+	Cl^-	5.62e-05	0.0221142	0.293881	8004790	0.0519778	*
OH^-	Na^+	2.26640e-06	2.658630e-02	0.797161	138833	3.3935e-02	*

* Parameters from previous works[1-3]
** Parameters regressed in this work

Table S4. Binary interaction parameters used in the short-range interaction term (Eq. S10)

Species *i*	Species *j*	$a_{ij}^{(0)}$	$a_{ij}^{(1)}$	$a_{ij}^{(2)}$	Source
HNO_3 (aq)	H_2O	5334.53	0	0	*
H_2O	TBP (aq)	-10742.89	71.1228	-0.10391	**
TBP (aq)	H_2O	6839.596	-36.08907	7.70e-02	**
HCl (aq)	H_3O^+	-5536.39	0	0	*
HCl (aq)	Cl^-	-5536.39	0	0	*
TBP (aq)	$Y(ClO_4)_3$TBP (aq)	-727.3686	-2.446115	0	**
$Y(ClO_4)_3$TBP (aq)	TBP (aq)	-623.4656	-2.115201	0	**
H_2O	$Y(ClO_4)_3$TBP (aq)	201.347	0	0	**
$Y(ClO_4)_3$TBP (aq)	H2O	195.8984	0	0	**
H_2O	$Y(Cl)_3$TBP (aq)	-8681.99	0	0	**
$Y(Cl)_3$TBP (aq)	H_2O	-7702.161	0	0	**
TBP (aq)	$Eu(Cl)_3$TBP (aq)	69055.41	0	0	**
$Eu(Cl)_3$TBP (aq)	TBP (aq)	-1580.904	0	0	**
TBP (aq)	$Eu(NO_3)_3$TBP (aq)	-77.64347	0	0	**
$Eu(NO_3)_3$TBP (aq)	TBP (aq)	-66.5388	0	0	**
TBP (aq)	$Y(Cl)_3$TBP (aq)	-12710.23	0	0	**
$Y(Cl)_3$TBP (aq)	TBP (aq)	-6489.671	0	0	**
ClO_4^-	TBP (aq)	19100.92	0	0	**
TBP (aq)	NO_3^-	62524.12	0	0	**
NO_3^-	TBP (aq)	106367.3	0	0	**
TBP (aq)	Cl^-	-1440.848	0	0	**
Cl^-	TBP (aq)	11748.64	0	0	**

* Parameters from previous works[1-3]
** Parameters regressed in this work

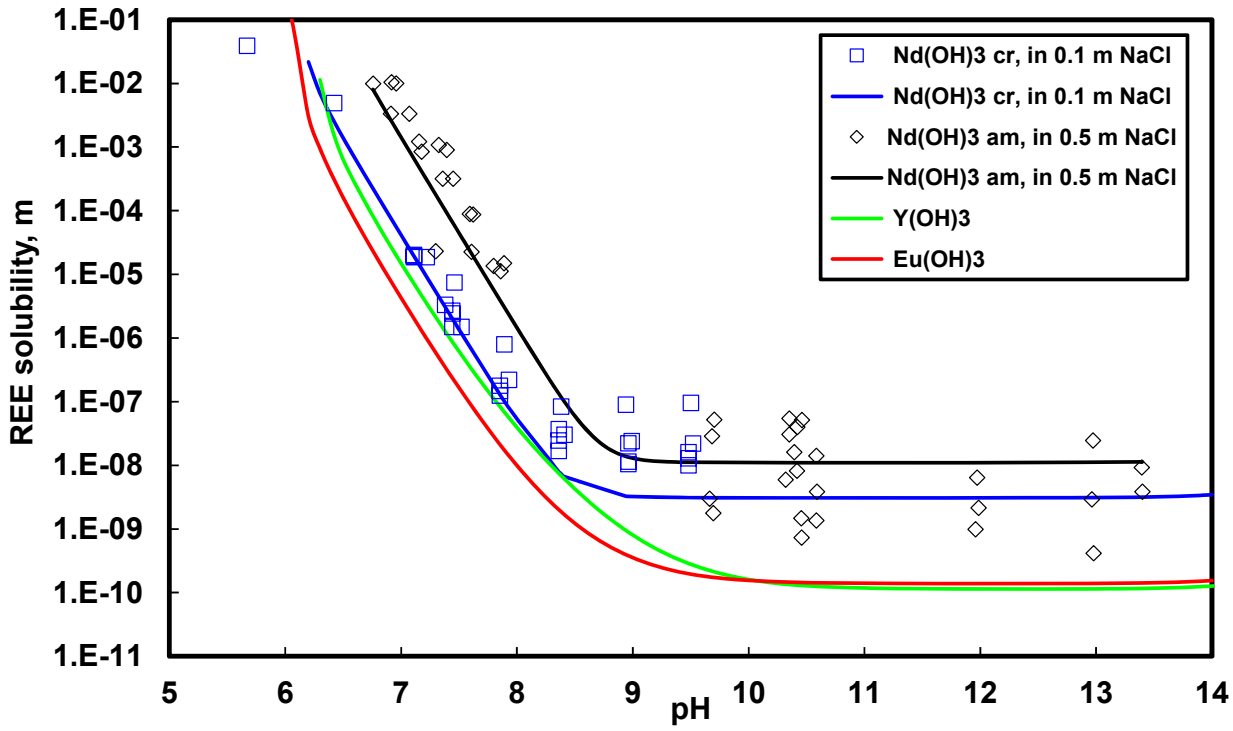

Figure S1. Solubility of REE hydroxides in aqueous solutions as a function of pH at 25°C. Symbols represent experimental solubility data of $Nd(OH)_3$: □,[23] in the presence of 0.1 m NaCl; ◊,[24] in the presence of 0.5 m NaCl. Curves indicate the calculated solubility values using the MSE thermodynamic model. cr: crystalline $Nd(OH)_3$; am: amorphous $Nd(OH)_3$.

References:

1. Wang, P.; Anderko, A.; Springer, R. D.; Young, R. D., Modeling Phase Equilibria and Speciation in Mixed-Solvent Electrolyte Systems: II. Liquid-Liquid Equilibria and Properties of Associating Electrolyte Solutions. *Journal of Molecular Liquids* **2006,** *125*, (1), 37-44.
2. Wang, P.; Anderko, A.; Young, R. D., A Speciation-Based Model for Mixed-Solvent Electrolyte Systems. *Fluid Phase Equilibria* **2002,** *203*, (1-2), 141-176.
3. Wang, P.; Springer, R. D.; Anderko, A.; Young, R. D., Modeling Phase Equilibria and Speciation in Mixed-Solvent Electrolyte Systems. *Fluid Phase Equilibria* **2004,** *222*, 11-17.
4. Pitzer, K. S., Electrolytes - from dilute solutions to fused salts. *Journal of the American Chemical Society* **1980,** *102*, (9), 2902-2906.
5. Abrams, D. S.; Prausnitz, J. M., Statistical thermodynamics of liquid mixtures - New expressions for excess Gibbs energy of partly or completely miscible systems. *AIChE Journal* **1975,** *21*, (1), 116-128.
6. Pitzer, K. S., *Thermodynamics, 3rd edition*. 3rd edition ed.; McGraw-Hill: New York, 1995.
7. Helgeson, H. C.; Kirkham, D. H.; Flowers, G. C., Theoretical prediction of the thermodynamic behavior of aqueous electrolytes at high pressures and temperatures. I Summary of the thermodynamic/electrostatic properties of the solvent. *American Journal of Science* **1974,** *274*, 1089-1198
8. Helgeson, H. C.; Kirkham, D. H.; Flowers, G. C., Theoretical Prediction of the Thermodynamic Behavior of Aqueous Electrolytes at High Pressures and Temperatures. II Debye-Hűckel Parameters for Activity Coefficients and Relative Partial Molal Properties. *American Journal of Science* **1974,** *274*, 1199-1261
9. Helgeson, H. C.; Kirkham, D. H.; Flowers, G. C., Theoretical Prediction of the Thermodynamic Behavior of Aqueous Electrolytes at High Pressures and Temperatures. III Equation of State for Aqueous Species at Infinite Dilution. *American Journal of Science* **1976,** *276*, 97-240
10. Helgeson, H. C.; Kirkham, D. H.; Flowers, G. C., Theoretical Prediction of the Thermodynamic Behavior of Aqueous Electrolytes at High Pressures and Temperatures. IV. Calculation of Activity Coefficients, Osmotic Coefficients, and Apparent Molal and Standard and Relative Partial Molal Properties to 5 kb and 600°C. *American Journal of Science* **1981,** *281*, 1241-1516.
11. Tanger, J. C.; Helgeson, H. C., Calculation of the thermodynamic and transport properties of aqueous species at high pressures and temperatures: Revised equations of state for the standard partial molal properties of ions and electrolytes. *American Journal of Science* **1988,** *288*, 19-98.
12. Haar, L.; Gallagher, J. S.; Kell, G. S., *NBS/NRC Steam Tables: Thermodynamic and Transport Properties and Computer Programs for Vapor and Liquid States in SI Units*. Hemisphere Publishing, Washington, DC: 1984.
13. Kosinski, J. J.; Wang, P. M.; Springer, R. D.; Anderko, A., Modeling Acid-Base Equilibria and Phase Behavior in Mixed-Solvent Electrolyte Systems. *Fluid Phase Equilibria* **2007,** *256*, (1-2), 34-41.
14. Siekierski, S., Extraction from solutions of perchloric acid by tributylphosphate—I: Partition coefficients for zirconium, thorium, cerium, promethium and yttrium. *Journal of Inorganic and Nuclear Chemistry* **1959,** *12*, (1), 129-135.
15. Levy, S. I., *The Rare Earths: Their Occurrence, Chemistry, and Technology*. E. Arnold: 1915.
16. Endres, G., Über die Basizität der seltenen Erden. *Zeitschrift für anorganische und allgemeine Chemie* **1932,** *205*, (4), 321-334.
17. Moeller, T.; Kremers, H. E., The Basicity Characteristics of Scandium, Yttrium, and the Rare Earth Elements. *Chemical Reviews* **1945,** *37*, (1), 97-159.
18. Shock, E. L.; Helgeson, H. C., Calculation of the Thermodynamic and Transport Properties of Aqueous Species at High Pressures and Temperatures: Correlation Algorithms for Ionic Species and

Equation of State Predictions to 5 kb and 1000°C. *Geochimica et Cosmochimica Acta* **1988,** *52*, 2009-2036.
19. Shock, E. L.; Helgeson, H. C.; Sverjensky, D. A., Calculation of the Thermodynamic and Transport Properties of Species at High Pressures and Temperatures: Standard Partial Molar Properties of Inorganic Neutral Species. *Geochimica et Cosmochimica Acta* **1989,** *53*, 2157-2183.
20. Shock, E. L.; Sassani, D. C.; Willis, M.; Sverjensky, D. A., Inorganic species in geologic fluids: correlations among standard molal thermodynamic properties of aqueous ions and hydroxide complexes. *Geochimica et Cosmochimica Acta* **1997,** *61*, (5), 907-950.
21. Haas, J. R.; Shock, E. L.; Sassani, D. C., Rare earth elements in hydrothermal systems: estimates of standard partial molal thermodynamic properties of aqueous complexes of the rare earth elements at high pressures and temperatures. *Geochimica et Cosmochimica Acta* **1995,** *59*, (21), 4329-4350.
22. Sako, T.; Hakuta, T.; Yoshitome, H., Vapor pressures of binary (water-hydrogen chloride,-magnesium chloride, and-calcium chloride) and ternary (water-magnesium chloride-calcium chloride) aqueous solutions. *Journal of Chemical and Engineering Data* **1985,** *30*, (2), 224-228.
23. Silva, R., The solubilities of crystalline neodymium and americium trihydroxides. *LBL-15055, Lawrence Berkeley National Laboratory, Berkeley, California* **1982**.
24. Neck, V.; Altmaier, M.; Rabung, T.; Lützenkirchen, J.; Fanghänel, T., Thermodynamics of trivalent actinides and neodymium in NaCl, MgCl2, and CaCl2 solutions: Solubility, hydrolysis, and ternary Ca-M (III)-OH complexes. *Pure and Applied Chemistry* **2009,** *81*, (9), 1555-1568.